



Optimization of the Propeller-Driven Propulsion System for a Small UAV

Nuno S. M. Moita and André C. Marta^(✉)

Center for Aerospace Science and Technology, IDMEC, Instituto Superior Técnico,
Universidade de Lisboa, Av. Rovisco Pais 1, 1049-001 Lisboa, Portugal
{nuno.moita, andre.marta}@tecnico.ulisboa.pt

Abstract. Integrated in the LEEUAV project, the objective of this work was to optimize the propeller-driven propulsion system previously implemented. A propeller was parametrized in terms of planform and airfoil shape and the software QPROP used to evaluate the performance of in terms of thrust, power and thrust coefficient and propeller efficiency. Experimental tests were conducted for three different propellers to study the performance sensitivity to propeller diameter and pitch, electric motors, and also to validate the numerical model. Following those tests, a multi-objective shape optimization using MATLAB[®], for cruise and climb conditions, was performed. At the end of this optimization, a system motor+propeller with an higher efficiency was obtained.

Keywords: Propeller · Optimization · Efficiency · Thrust
Electrical power

1 Introduction

The propeller-driven propulsion system designed in this work will be implemented in the Long Endurance Electrical Unmanned Aerial Vehicle (LEEUAV) project, developed by AeroG/UBI, IDMEC/IST and INEGI/FEUP, whose ultimate goal is to produce a low-cost, long-endurance UAV for flexible surveillance missions [12].

The first step is to select a software for numerical simulations of the performance data of a given system motor+propeller and to parametrize the propeller shape. Then, wind tunnel tests will be made to predict to validate the performance prediction of the numerical software for different motor+propeller systems. Having completed that, an optimization tool will be built, based on the validated numerical software, to determine the optimized propeller shape and operating conditions for prescribed climb and cruise mission stages. At the end, it is intended to fabricate the obtained optimized propeller by means of additive manufacturing.

2 Analytical Propeller Analysis

There are several models used to perform propeller analysis such as the actuator disk theory, the lifting line theory, the vortex lattice model and the panel method. However, the most common are the Blade Element Theory (BET) and the Blade Element Momentum Theory (BEMT).

2.1 Propeller Analysis Models

The BET [14] is a simple and fast method that consists in splitting each blade in independent sections which are analysed based on the local velocities. At each section, a 2D force balance is applied to obtain lift, drag, thrust and torque distributions. A final integration over the entire blade gives the performance characteristics of the blade. The flow is analyzed independently on each section assuming there are only axial and angular velocities and there is no induced flow from any other sections. The propeller thrust and torque are then obtained by integrating these 2D elements over the blade radius. Due to this simplicity, it does not account the effect of the induced velocities on the blades, swirl in the slipstream, non-uniform flow, or propeller blockage.

The BEMT corresponds to an upgrade of the BET where the induced velocities are taken in account, including both the lift-induced and the externally-induced velocities, at the expense of additional complexity.

2.2 Propeller Parametrization

Three categories of parameters are used to define the propeller: planform shape; airfoil characteristics; and performance.

The planform shape of the propeller is defined by the diameter D , the chord distribution $c(r)$ and the pitch angle distribution $\beta(r)$.

The airfoil characteristics used in the software to determine the lift curve and the drag polar include: the maximum lift coefficient $C_{l_{max}}$, the minimum lift coefficient $C_{l_{min}}$, the lift coefficient at zero angle of attack C_{l_0} , the lift coefficient derivative with the angle of attack C_{l_α} , the profile drag coefficient C_{d_0} and corresponding the lift coefficient $C_{l_{C_{d_0}}}$, the drag coefficient slope C_{l_2} , the reference Reynolds number Re_{ref} and the Reynolds exponent that adjusts the polar for other Reynolds numbers, Re_{expo} .

The performance parameters include the thrust coefficient C_T relates the thrust produced by a propeller with its diameter and rotation velocity, and the power coefficient C_P relates the mechanical power produced by a propeller with its diameter and rotation velocity, respectively as

$$C_T = \frac{T}{\rho N^2 D^4}, \quad C_P = \frac{P_{shaft}}{\rho N^3 D^5}. \quad (1)$$

Also important is the propeller efficiency η , here defined as the ratio between the mechanical power that a propeller can use and the electrical power P supplied to the system,

$$\eta = \frac{TU}{P}. \quad (2)$$

A common dimensionless parameter used in propellers is the advance ratio, J , that relates the velocity with the rotation velocity and the diameter of a propeller, $J = \frac{U}{ND}$.

3 Numerical Propeller Analysis

Several propeller analysis softwares were studied, namely AKPD/AKPA [2], JavaProp [6] and QPROP [5]. In the end, the latter was chosen not only given its capability to predict the desired propulsive performance outputs for a given combination of motor+propeller system, and also for its simple integration in MATLAB[®] for the optimization framework to be developed.

To execute QPROP, two main files are necessary: the motor file where the motor parameters are defined, and the propeller file where the planform shape and airfoil parameters are defined.

4 Experimental Facility

4.1 Electric Motors

Two DC brushless electrical motors were considered, the OS-3810-1050 and the OS-5020-490 [11], whose characteristics are presented in Table 1, where I_0 is the zero-load current, I_{max} is the maximum current supported by the motor, η_{max} is the maximum efficiency the motor can reach, K_v is the motor constant and R is the internal resistance of the motor.

Table 1. Characteristics of the electric motors

Motor	V^* [V]	I_{max} [A]	I_0 [A]	η_{max} [%]	K_v [RPM/V]	R [m Ω]
OS-3810-1050	12.5	30	1.1	85	1050	51.3
OS-5020-490	21.0	68	1.5	85	490	23

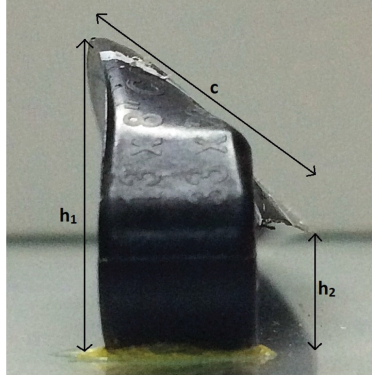
4.2 Propellers

Three different propellers with varying diameter and pitch were analyzed, all from APC [1], as summarized in Table 2. The first number in propeller designation refers to the blade diameter and the second to the blade pitch, both in inches.

Due to the non-existence of geometry details of any of the propellers to be tested, it was necessary to find a way to measure their planform shape. It was first tried a 3D scanning with a laser scanner but it showed to be very inaccurate due to the inaccuracy of the measuring laser system. As such, manual measurement

Table 2. Characteristics of propellers tested

Propeller	c_{avg} [mm]	R [mm]	Re
APC 13" \times 8"	17.5	145	94,416
APC 16" \times 8"	20.4	183	138,908
APC 16" \times 10"	21.2	180	142,073


Fig. 1. Scheme of the measurement procedure of the propeller blade

proved to be the most reliable, in which the blade was marked at several sections and the chord c and heights h_1 and h_2 measured with a caliper of each section k , as illustrated in Fig. 1. The twist distribution β as a function of the section was then computed as $\beta_k = \arcsin \frac{h_{1k} - h_{2k}}{c_k}$.

To predict the performance of a propeller, it was also necessary to determine the airfoil parameters. To calculate the Reynolds number for the analysis, standard sea-level atmospheric conditions and a propeller speed of 5,000 RPM were considered. Since it was desired to have a unique Reynolds number for all propellers, it was decided to set $Re = 100,000$. Knowing that the airfoils used were the Clark-Y or the NACA 4412 [1], the parameters of each one were calculated using the software XFOIL, from which it was possible to define the propeller files to be used in QPROP.

4.3 Force Balance

To obtain the desired data for the determination of the parameters of the propeller, it was necessary to perform static and dynamic tests in the wind tunnel, using a force balance [4] to measure the motor+propeller system parameters. This measuring system can be observed in Fig. 2.

To measure the loads applied in the system, two different load cells were used, depending on the motor+propeller system. To assure the accuracy of the measured values, every sensor has to be calibrated. For illustration, the regressions obtained for the load cells, motor voltage and current, and airspeed sensors are shown in Fig. 3.



Fig. 2. Force balanced to characterize the motor+propeller system

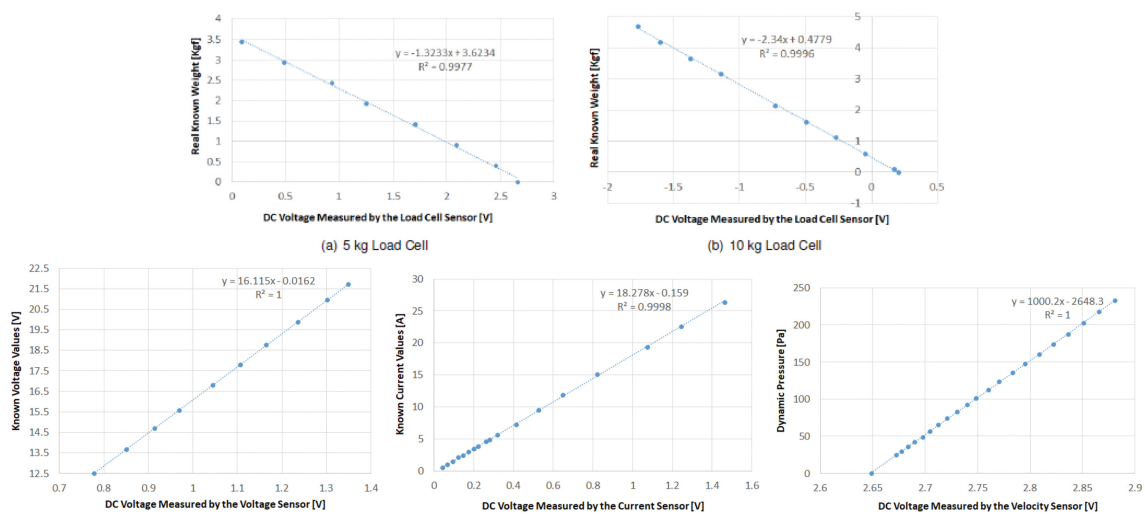


Fig. 3. Linear regressions used to calibrate the force balance sensors

5 Baseline Propeller Analysis

After preparing the experimental facility, tests were performed using the force balance described. In these tests, several parameters were analyzed for each combination of motor and propeller, for different electrical conditions, in particular thrust, electrical power, thrust coefficient, power coefficient and efficiency.

5.1 LEEUAV Case Study

After performing the experimental tests, it was analyzed the best way to apply the results to the case in study, the LEEUAV. In [13], several flight tests were performed in cruise conditions, which is bar far the longest stage, which allowed to determine the value of required thrust for a given airspeed. Since the efficiency for each airspeed and thrust were determined in the experimental tests, it was possible to analyze the propeller efficiency variation of a given propeller+motor system by applying the LEEUAV cruise flight conditions. This process was

important since it was possible, before any optimization, to verify which system would be the most efficient for the LEEUAV.

The parameters taken in account were the propeller diameter and pitch, the electric motor and the input voltage. The experimental propeller efficiency variation for each system obtained for cruise conditions is shown in Fig. 4. It is possible to conclude that: the motor OS-3810-1050 is the most efficient for velocities under 9.57 m/s; the higher the diameter, the higher the efficiency; the higher the pitch, the higher efficiency and the higher the input voltage, the lower the efficiency. Since the LEEUAV cruises at 7.53 m/s, the most efficient system to implement would be the OS-3810-1050, attached to the APC 13" × 8" propeller, powered at 12.5 V.

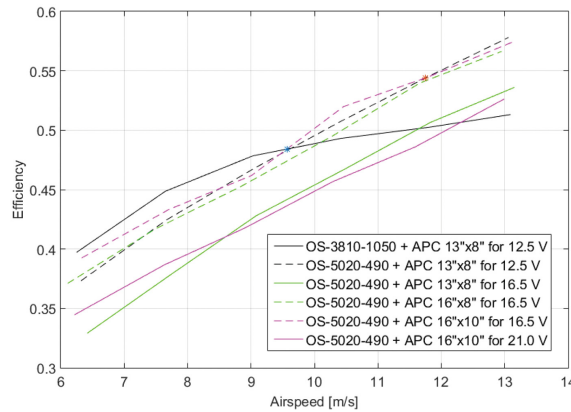


Fig. 4. Comparison of the variation of efficiency with airspeed for all systems

The variation of the thrust coefficient C_T and the power coefficient C_P with the advance ratio J was also studied and compared with the literature [8], as shown in Fig. 5. Both coefficients decrease with the increase of the advance ratio that although the curves exhibit similar behavior, the experimental values are lower relatively to the literature, which means that the estimated blade twist angles were probably higher than the real ones.

5.2 Analysis Framework and Validation Procedure

To obtain the simulations data, a routine in MATLAB[®] called “Analysis Framework” was developed, that would later facilitate the construction of the optimization framework, allowing the user to provide the required inputs and then to present the outputs, as schematically shown in Fig. 6.

After obtaining the experimental results, it was possible to compute the numerical results using the software QPROP. However, at this stage, it was important to assure the highest level of accuracy of the numerical model, that would later be used in the optimization process. To perform the validation, the *Least Squares Fitting* method [3] was used, where the residual was given by

$$Residual = \sum (y_{exp} - y_{num})^2. \quad (3)$$

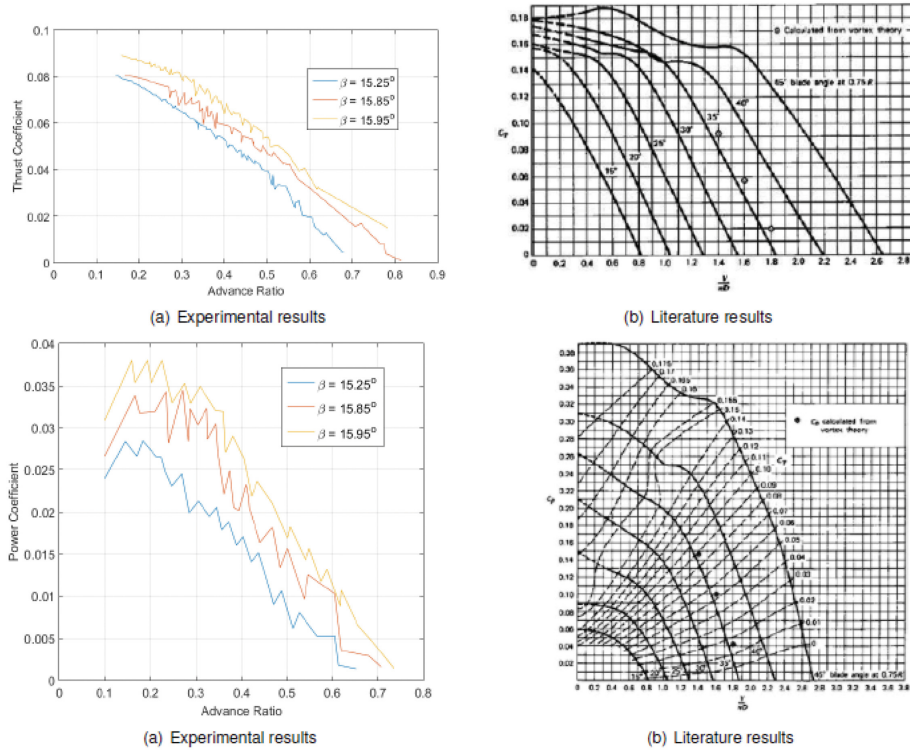


Fig. 5. Variation of thrust and power coefficients with advance ratio

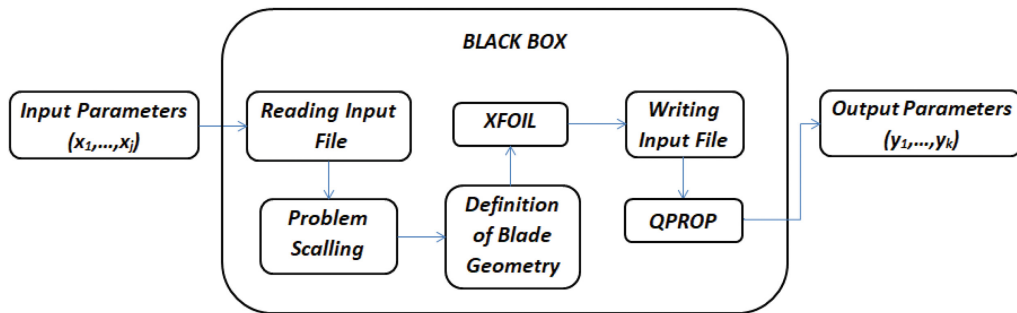


Fig. 6. Analysis framework for propeller+motor system simulations

The parameters used in the validation were the offset added to the β distribution of the blades, β_{add} , that had been initially manually measured, and the internal resistance of the motor, R . These two parameters affect the estimated thrust and electrical power, respectively. Tables 3 and 4 present the parameters obtained in this validation.

Table 3. Validated characteristics for each propeller

Propeller	Airfoil	$\beta_{add} [^\circ]$
13" × 8"	NACA 4412	0.58
16" × 8"	Clark-Y	-0.5
16" × 10"	Clark-Y	-1.07

Table 4. Validated internal resistance for each motor

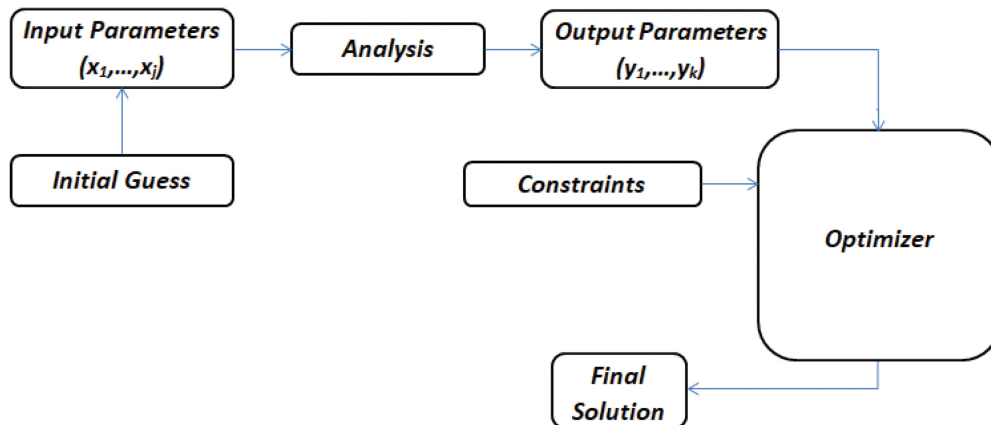
Motor	Resistance [$m\Omega$]
OS-3810-1050	75.9
OS-5020-490	88.5

6 Propeller Optimization

6.1 Process Description

Before using the optimization algorithm, it is necessary to properly define the optimization problem, which encompasses the objective function, the design variables, bound constraints, linear and non-linear constraints.

A gradient-based optimization algorithm was selected, in particular an interior-point algorithm, suited for constrained problems with smooth functions [10]. Because QPROP only exports discrete results, a relative step size factor was set to define the perturbation step in the finite differences approximations to the function gradients. This step size was selected for each design variable after a sensitivity study was performed.


Fig. 7. Optimization process scheme

A flowchart describing the entire optimization process is presented in Fig. 7.

The system used as a starting point in this process was the OS-3810-1050 with the APC 13" × 8" modeled with the NACA 4412 airfoil, corresponding to

the legacy LEEUAV propulsion system. The optimization process was performed for climb and cruise conditions considering airspeeds of 7.67 m/s and 7.53 m/s, respectively.

6.2 Planform Optimization

After analyzing the parameters that would have a larger impact on the propeller performance, it was decided that the objective of the optimization problem was to optimize the propeller efficiency, Eq. (2). However, it was desired to optimize the efficiency for both flight stages, η_{cruise} and η_{climb} , corresponding to the cruise and climb conditions, respectively. Since it was only intended to generate one optimum propeller, a final objective function was created that corresponds to efficiency of the entire flight, using a multi-objective optimization with the weighted aggregation method described in [9] as

$$\epsilon = \frac{E_{cruise}}{E_{cruise} + E_{climb}}, \quad (4)$$

where E_{cruise} is the total energy spent by the UAV in cruise and E_{climb} is total energy spent by the UAV during the climb. According to [7], the required energy during climb is 266.9 kJ and the required energy during cruise is 1370.9 kJ, which means that $\epsilon = 0.837$. As such, it was possible to build the objective problem as

$$\eta_{total} = 0.837\eta_{cruise} + 0.163\eta_{climb}, \quad (5)$$

The optimization problem could then be posed as

Maximize $\eta_{total} = F(\mathbf{x}_{total})$

w.r.t. $\mathbf{x}_{total} = (\beta_1, \beta_2, \beta_3, \beta_4, c_1, c_2, c_3, c_4, R, RPM_{cruise}, RPM_{climb})$

subject to $\mathbf{x}_{0total} = (90, 23, 14, 0.3, 7, 24, 13, 1.2, 150, 3550, 6250)$ (6)

$\mathbf{lb}_{total} = [87, 22, 13, 0, 6, 22, 12, 1, 145, 3500, 6200]$

$\mathbf{ub}_{total} = [90, 24, 15, 0.5, 9, 25, 15, 2.1, 184, 3700, 6400]$

where \mathbf{x}_{total} is the design variables vector, \mathbf{x}_{0total} is the initial guess of the design variables vector, \mathbf{lb}_{total} and \mathbf{ub}_{total} are the lower and upper bound constraints, respectively, R is the propeller radius, RPM_{cruise} and RPM_{climb} are the RPM for cruise and climb conditions, respectively, R is the propeller radius and $\beta_1, \beta_2, \beta_3, \beta_4$ and c_1, c_2, c_3, c_4 are the four equidistant control points used to build the cubic spline for $\beta(r)$ and $c(r)$ distributions respectively, as shown in Fig. 8.

According to Fig. 4, a minimum value for thrust at cruise of 3.57 N was obtained. For climb conditions, the minimum value of thrust is 13.88 N. Since for an input voltage of 12.5 V, it was only possible to obtain a maximum current of 30 A in safe conditions, it was decided to limit the maximum electrical power

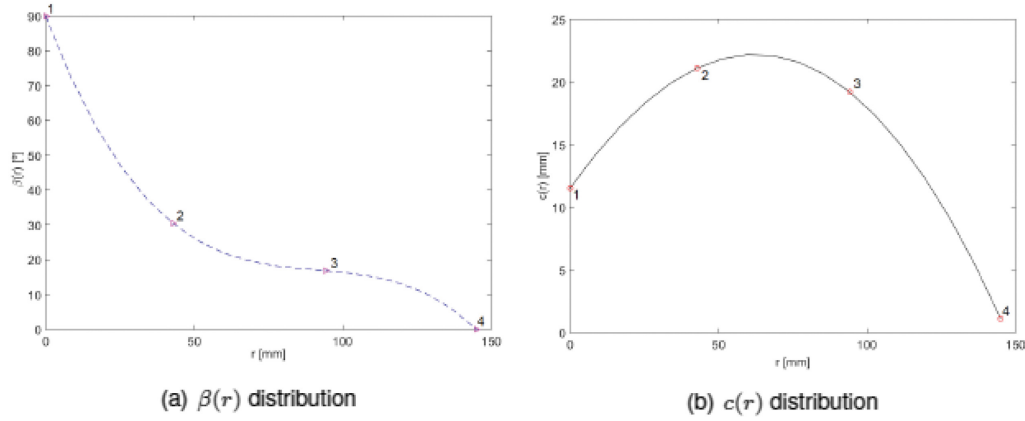


Fig. 8. Bezier control points doe the propeller twist and chord distribution

of the motor to 375 W. Consequently, to assure that these requirements were fulfilled, nonlinear constraints were added to Eq. (6) in the form

$$\begin{aligned} C_1 &= 3.57 - T_{cruise} \\ C_2 &= 13.88 - T_{climb} \\ C_3 &= P - 375. \end{aligned} \quad (7)$$

Upon convergence of the optimization of optimization process, the optimum blade radius, R , found was 168.5 mm. Figures 9 and 10 show the initial and the optimum propeller twist $\beta(r)$ and chord $c(r)$ distributions.

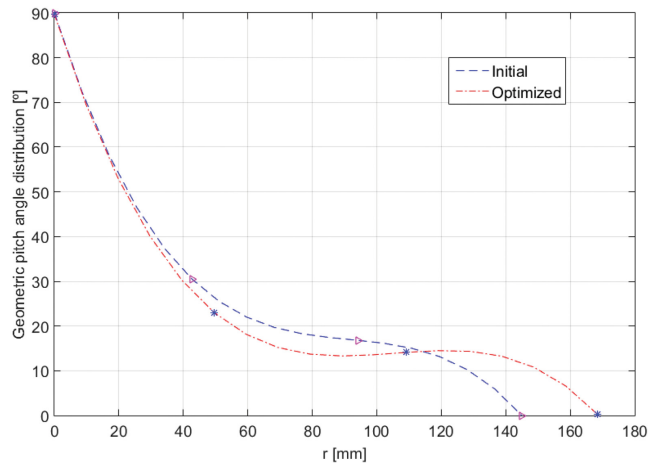


Fig. 9. Geometric pitch angle distribution of the propeller blade

The results between the performance of the initial propeller and the final propeller are presented in Table 5. The total efficiency increased 42.53% to $\eta_{total} = 43.34\%$, representing savings in energy of 244.8 kJ for climb conditions and 1356.52 kJ cruise conditions. This optimized propeller-driven system is thus expected to allow for an additional 9 min of flight time, if the energy sources remain constant.

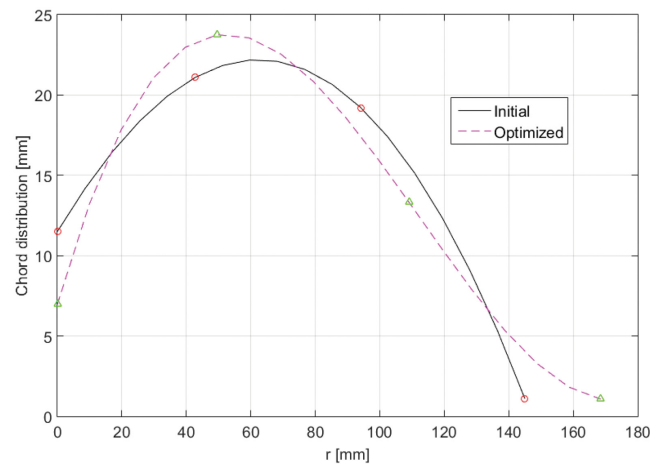


Fig. 10. Chord distributions propeller blade

Table 5. Comparison of the results obtained for the initial and the final propeller

Flight stage	U [m/s]	RPM	T [N]	C_T	C_P	J	P [W]	η [%]
Climb - initial	7.67	5934	13.88	0.0867	0.0433	0.2301	375.2	28.38
Climb - final	7.67	6270	13.88	0.0462	0.0185	0.218	344.1	30.94
Cruise - initial	7.53	3317	3.57	0.0714	0.0435	0.4042	59.36	45.28
Cruise - final	7.53	3610	3.57	0.036	0.018	0.371	58.77	45.76

6.3 Optimal Propeller Prototype

After the optimization process completed, a new propeller file was obtained with the detailed geometry distribution parameters. To obtain the tridimensional model, it was necessary to determine the coordinates of the points for each section k . These points were calculated according to

$$\begin{bmatrix} \mathbf{x}_k^* \\ \mathbf{y}_k^* \end{bmatrix} = c_k \times \begin{bmatrix} \cos \beta_k & \sin \beta_k \\ -\sin \beta_k & \cos \beta_k \end{bmatrix} \times \begin{bmatrix} \mathbf{x}_k \\ \mathbf{y}_k \end{bmatrix} \quad (8)$$

where \mathbf{x}_k and \mathbf{y}_k are the vectors of coordinates of the original profile, \mathbf{x}_k^* and \mathbf{y}_k^* are the new coordinates of the airfoil and c_k is the chord value for each section of the blade. After having all the points on the rotated referential for each section, a tridimensional model of the propeller was designed using SOLIDWORKS[®].

After modeling the blade, the model was printed in PLA using a 3D-printer, with a filament diameter of 0.4 mm. The final prototype model of the optimized blades can be visualized in Fig. 11.

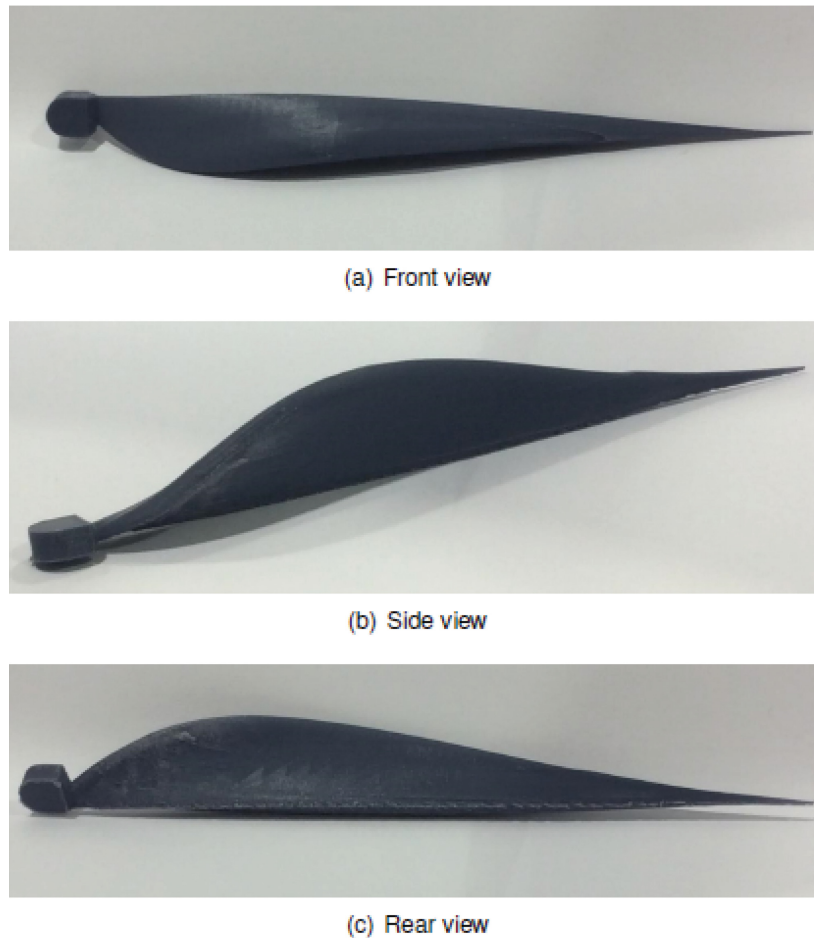


Fig. 11. Optimal propeller blade prototype

7 Conclusions

A propeller optimization framework was developed based on the analysis tool QPROP and optimization tools from MATLAB[®].

Experimental tests were performed not only to validate the numerical model but also to assess the sensitivity of propulsive efficiency, defined as the ratio between the mechanical power delivered by the propeller and the electrical power supplied to the system. Given the knife like geometry of the propeller blades, it was found to be impractical the use of laser scanning for the geometry measurements. Instead, a manual procedure emerged has the most reliable method. The validation tests allowed to match the estimated thrust and efficiency by means of the correction in the measured twist distribution using an offset parameter β_{add} , and the correction of the electric motor internal resistance R .

After performing the experimental tests and applying the gathered data to the specific case of the LEEUAV, it was concluded that the use of the motor OS-3810-1050 was more efficient for airspeeds below 9.57 m/s; the higher the diameter and the pitch of a propeller, the higher the efficiency and that the efficiency decreases with the increase of the input voltage.

Since it was only intended to design a single propeller, a multi-objective optimization using the weighted aggregation method was performed. The weights in the multi-objective function considered the ratio of energy consumed in each flight stage, climb and cruise, compared to the total energy consumed. The resulting optimized propeller was then a trade-off between flight stages.

Remarkably, the optimization process led to a propeller design with increased efficiency for each flight stages, which consequently resulted in an increase of the total efficiency of the flight. This new design is expected to allow for an increase of 9 min in flight time for the LEEUAV, which represents about 1.5% extension.

At the end, the new blade was virtually drawn using the SOLIDWORKS[®] and then built using additive manufacturing techniques, namely a rapid prototyping 3D printer with PLA, with a diameter filament of 0.4 mm.

Future work will include the experimental test of the newly designed blade to validate its performance. This will imply the choice of a different building material that is found safe for testing at high rotational speeds.

References

1. APC Propellers: Propeller performance data (2017). <https://www.apcprop.com/>. Accessed May 2017
2. Berg, A.: AKPD/AKPA (2003). https://www.sintef.no/globalassets/upload/marintek/pdf-filer/software/akpd-akpa_programpackage.pdf. Accessed Mar 2018
3. Bevington, P.R.: Data Reduction and Error Analysis for the Physical Sciences. McGraw-Hill, New York (1969). ISBN:0-07-247227-8
4. Borges, M.: Design of an apparatus for wind tunnel tests of electric UAV propulsion systems. Master's thesis, Instituto Superior Técnico, Universidade de Lisboa (2015)
5. Drela, M.: QPROP formulation (2006). http://web.mit.edu/drela/Public/web/qprop/qprop_theory.pdf
6. Hepperle, M.: JavaProp - user guide (2018). <http://www.mh-aerotoools.de/airfoils/javaprop.htm>. Accessed Mar 2017
7. Marta, A.C., Gamboa, P.V.: Long endurance electric UAV for civilian surveillance missions. In: 29th Congress of International Council of the Aeronautical Sciences (2014)
8. McCormick, B.W.: Aerodynamics Aeronautics and Flight Mechanics, 2nd edn. Pennsylvania State University, State College (1995). ISBN:0-471-5706-2
9. Ngatchou, P., Zarei, A., El-Sharkawi, M.A.: Pareto multi objective optimization. In: Intelligent Systems Application to Power Systems, pp. 84–89 (2005). <https://doi.org/10.1109/ISAP.2005.1599245>
10. Nocedal, J., Wright, S.J.: Numerical Optimization, 2nd edn. Springer, New York (1999). ISBN:0-387-30303-0
11. Engine, O.S.: Brushless motors (2017). <https://www.osengines.com/>. Accessed Feb 2017
12. Parada, L.M.A.: Conceptual and preliminary design of a long endurance electric UAV. Master's thesis, Instituto Superior Técnico, Universidade de Lisboa (2016)
13. Rodrigues, A.: Airframe assembly, systems integration and flight testing of a long endurance electric UAV. Master's thesis, Universidade da Beira Interior (2017)
14. Roskam, J.: Airplane Aerodynamics and Performance, 1st edn. DARcorporation, Lawrence (1997). ISBN:1-884885-44-6